Bull. Mater. Sci., Vol. 31, No. 5, October 2008, pp. 753–758. © Indian Academy of Sciences.

p-$AgCoO_2$/*n*-ZnO heterojunction diode grown by rf magnetron sputtering

K A VANAJA, UMANANDA M BHATTA[†], R S AJIMSHA, S JAYALEKSHMI and M K JAYARAJ*

Department of Physics, Cochin University of Science and Technology, Kochi 682 022, India

[†]Institute of Physics, Bhubaneswar 751 005, India

MS received 19 December 2007; revised 25 March 2008

Abstract. ***P*-type transparent semiconducting $AgCoO_2$ thin films were deposited by rf magnetron sputtering of sintered $AgCoO_2$ target. The $AgCoO_2$ films grown by rf sputtering were highly *c*-axis oriented showing only (001) reflections in the X-ray diffraction pattern unlike in the case of amorphous films grown by pulsed laser deposition (PLD). The bulk powder of $AgCoO_2$ was synthesized by hydrothermal process. The optical bandgap was estimated as 4·15 eV and has a transmission of about 50% in the visible region. The temperature dependence of conductivity shows a semiconducting behaviour. The positive sign of Seebeck coefficient (+220 μVK^{-1}) indicates *p*-type conductivity. Transparent *p–n* heterojunction on glass substrate was fabricated by rf magnetron sputtering of *p*-$AgCoO_2$ and *n*-type ZnO : Al thin films. The structure of the diode was glass/ITO/*n*-ZnO/*p*-$AgCoO_2$. The junction between *p*-$AgCoO_2$ and *n*-ZnO was found to be rectifying.**

Keywords. **rf sputtering; *p–n* junction; *p*-type; HRTEM.**

1. Introduction

Transparent semiconducting oxides (TSO) have attracted attention for their application to optoelectronic devices especially for blue and UV emitters. Optically transparent oxides with large bandgap are intrinsically insulators. Most of the transparent conducting oxides which are being commercially used are of *n*-type. Wide bandgap oxides like In_2O_3:Sn (ITO), ZnO, SnO_2 etc have widely been investigated for the past four decades. The use of TSOs in the fabrication of optoelectronic devices did not materialize due to lack of TSO that exhibit *p*-type conductivity. In 1997, Kawazoe *et al* reported the *p*-type conducting transparent $CuAlO_2$ films. This was followed by a number of reports of improved *p*-type conductivity in a number of related delafossite materials such as $CuMO_2$ (M = Al, Ga, In, Y, Sc) (Duan *et al* 2000; Jayaraj *et al* 2001; Ueda *et al* 2001; Yanagi *et al* 2001b; Banerjee and Chattopadhyay 2005) and $AgInO_2$ (Subrahmanyam and Barik 2005). All oxide transparent *p–n* junction and ultra violet emitting diode (Ohta *et al* 2000) was successfully fabricated using ZnO and $SrCuO_2$. Rectifying behaviour in other oxide based structures has also been reported including *p*-NiO/*i*-NiO/*i*-ZnO/*n*-ZnO (Sato *et al* 1993), *n*-ZnO/*p*-ZnO (Aoki *et al* 2000) and *p*-$CuYO_2$/*i*-ZnO/*n*-ZnO (Hoffman *et al* 2001). $CuInO_2$ is the only delafossite structure known to exhibit bipolar conductivity and homojunction $CuInO_2$: Sn/$CuInO_2$: Mg has been fabricated (Yanagi *et al* 2001a). Wide bandgap semiconductors are difficult to dope, particularly, the *p*-type (Nie *et al* 2002). Despite the interest in delafossite material, silver delafossite films are less investigated. The $AgInO_2$: Sn has been reported to show *n*-type conductivity and *p*-type doping was unsuccessful (Otabe *et al* 1998). It has been reported that Ag_xCoO_2 ($x < 1$) powder synthesized by ion exchange has *p*-type conductivity due to 3*d* type holes mixed with O 2*p*-ligand holes (Jshin *et al* 1997; Kng *et al* 2002). In this work, $AgCoO_2$ has been synthesized by hydrothermal method. The electrical and optical properties of the $AgCoO_2$ thin film and rectifying nature of *p*-$AgCoO_2$/*n*-ZnO junction are reported.

*Author for correspondence (mkj@cusat.ac.in)

2. Experimental

In the present study, $AgCoO_2$ powder was prepared by four-day hydrothermal reaction in a parr bomb at 250°C. The reagents used were $AgNO_3$, Co_3O_4 and KOH. A 2 inch diameter sputtering target was prepared by pelletizing and heating the powder at 350°C for 5 h in air. The $AgCoO_2$ films were sputtered in an axis geometry in 80 : 20; Ar : O_2 mixture at 40 mtorr. The substrates were single crystal Al_2O_3 or amorphous silica placed at 4 cm from target and heated to 400°C. The thickness of the films were measured using a stylus profiler (Dektak 6 M). The structural properties were studied by X-ray diffraction using Rigaku D-max X-ray diffractometer with CuK_α line. The high resolution transmission electron micrographs (HRTEM) and selective area electron diffraction (SAED) patterns were recorded using model JEM-2010 UHR of JEOL at an operating voltage of 200 keV. The composition of the films was analysed using the electron probe micro analysis (EPMA). The electrical conductivity was measured in the van der Pauw configuration using the hall measurement setup. The thermo power measurements were carried out using a home made automated setup (Manoj *et al* 2003). Transparent *p–n* heterojunction fabricated have the structure: glass/ITO/*n*-ZnO/*p*-$AgCoO_2$. The *J–V* characteristics were evaluated by applying d.c. voltage to the diode using a Keithley source measure unit (SMU 236). Indium metal was used as the ohmic contacts. The glass substrate was coated with sputtered (Nisha *et al* 2005) 200 nm thick ITO at a substrate temperature of 150°C. ZnO : Al was deposited on the ITO coated glass substrate by rf magnetron sputtering at a substrate temperature of 150°C in an argon pressure of 10 mtorr (Jayaraj *et al* 2002). *p–n* junction of area, $7{\cdot}05 \times 10^{-2}$ cm^2, was completed by depositing $AgCoO_2$ through a shadow mask on glass/ITO/ZnO : Al structure.

3. Results and discussion

X-ray diffraction pattern of the hydrothermally synthesized $AgCoO_2$ powder is shown in figure 1(a). All the peaks can be indexed by assuming a 6H polytype delafossite structure (Stahlin *et al* 1970). However, an actual 6H delafossite structure has not been proposed and the observed diffraction pattern can be accounted for a mixture of 2H and 3R forms, a situation commonly observed for delafossite compounds. From EPMA, Ag : Co ratio is obtained as 1·2 : 1. The $AgCoO_2$ film grown on Al_2O_3 substrate as well as on glass substrate was *c*-axis oriented, as only the (00l) diffraction peaks were visible (figure 1(b)). All diffraction peaks were identified as that of $AgCoO_2$. The selective area electron diffraction pattern (SAED) of the hydrothermally grown $AgCoO_2$ powder is shown in figure 2(a). The lattice spacing corresponding to the diffraction pattern was determined with camera constant of the equipment and measuring the radius from the electron diffraction pattern (Hirsch *et al* 1977). Diffraction spots corresponding to (110) and (0012) planes of delafossite structure of $AgCoO_2$ were observed. SAED of sputtered $AgCoO_2$ film shows the diffraction spots representing the (012) and (0012) planes (figure 2(b)). The nature of the substrate influences the growth and crystal structure of the film. The orientation of the films grown on silica and carbon coated grids may be different, however, the same deposition conditions as that of $AgCoO_2$ grown on silica leads to the crystalline $AgCoO_2$ films without any impurity phase. The trials to grow crystalline Ag-CoO_2 films by pulsed laser deposition (PLD) was unsuccessful (Ajimsha *et al* 2007). The PLD resulted in the amorphous films even on the single crystalline substrate. In the present study, highly *c*-axis oriented $AgCoO_2$ films were able to grow by rf magnetron sputtering. However, *p*-$AgCoO_2$/*n*-ZnO heterojunction grown by rf magnetron sputtering had similar characteristics as in the case of PLD grown junction (figure 8). The *n*-ZnO is deposited at reducing atmosphere which generates oxygen vacancies and *n*-type carriers. *p*-$AgCoO_2$ is deposited at 400°C under an oxygen pressure to induce *p*-type conductivity. There is a possibility of growing very thin intrinsic ZnO layer during the deposition of *p*-$AgCoO_2$ at elevated temperature in the presence of oxygen. The diode characteristics in the present case is dominated by the interface states. This may be the reason for similar diode characteristics for the junctions fabricated by PLD and rf magnetron sputtering even though there is a drastic improvement in crystallinity for films grown by magnetron sputtering. Also the junction current observed in the case of PLD grown amorphous junctions is higher than the junctions grown by sputtering. A 150 nm $AgCoO_2$ film shows 40–60% transparency in the visible region while ZnO film gives a transmission of 85% (figure 3). The bandgap of $AgCoO_2$ films were obtained by plotting the absorption coefficient, α, as a function of frequency. Extrapolating the straight line portion of $(\alpha h\nu)^2$ vs $h\nu$ plot to the energy axis yields the bandgap (E_g) and the exponent gives information about the nature of optical bandgap (Yu and Cardona 1996). Bandgap of $AgCoO_2$ film was estimated to be 4·15 eV (figure 4). The bandgap of $AgCoO_2$ powder sample was estimated by recording the diffuse reflectance spectrum of the samples in the visible region using MgO as the reference. The bandgap was found to be ~3·96 eV estimated from the plot of $\{(k/s)/h\nu)^2\}$ vs $h\nu$ (inset of

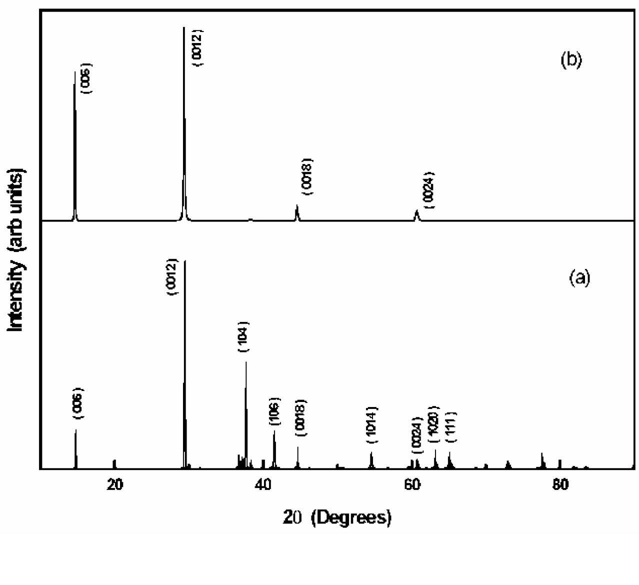

Figure 1. X-ray diffraction patterns of (a) $AgCoO_2$ powder and (b) $AgCoO_2$ thin film.

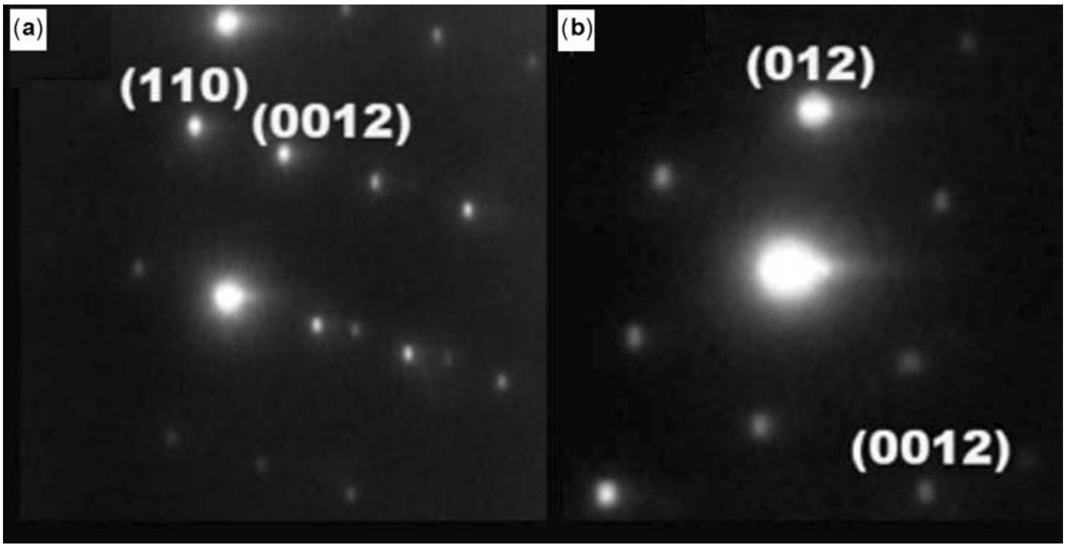

Figure 2. (**a**) SAED of hydrothermally grown $AgCoO_2$ powder and (**b**) $AgCoO_2$ thin film grown on carbon coated copper grid.

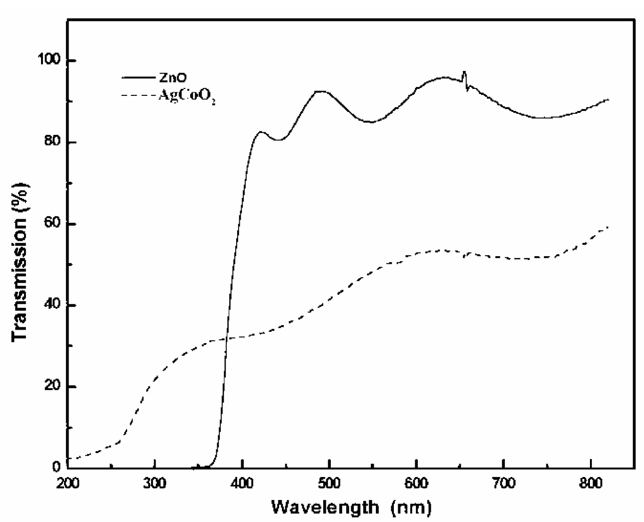

Figure 3. Transmission spectra of $AgCoO_2$ and ZnO thin films.

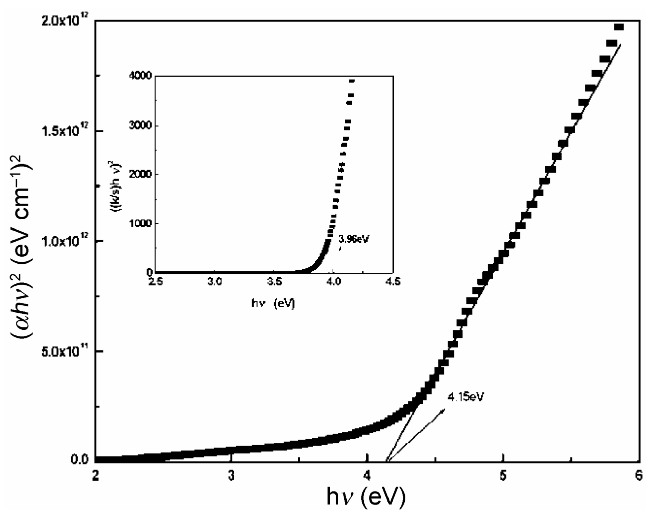

Figure 4. $(\alpha h\nu)^2$ vs $h\nu$ plot of $AgCoO_2$ thin film and inset shows the $((k/s)h\nu)^2$ vs $h\nu$ plot of $AgCoO_2$ powder.

figure 4), where k and s denote the absorption and scattering coefficients and $h\nu$ the photon energy. The ratio of k/s was calculated from the reflectance spectra via Kubelka–Munk equations (Kubelka and Munk 1931; Kubelka 1948). The temperature dependence of resistivity shows a semiconducting behaviour. The activation energy extracted from the slope of $\log\sigma$ vs $1000/T$ plot is 70 meV at high temperature. The room temperature conductivity is 0·2 Scm^{-1}. The $\log(\sigma)$ vs $1000/T$ plot is not well fit by a single line (figure 5). However, the $\log(\sigma T^{1/2})$ vs $1/T^{1/4}$ plot (inset of figure 5) is close to a straight line suggesting that a variable range hopping (Mott 1974) is dominant in positive hole conduction at the top of valence band which is observed in similar delafossite materials (Duan *et al* 2000; Jayaraj *et al* 2001). The Ag^+ ions contributing to the conductivity in thin film of $AgCoO_2$ has been estimated by measuring the transference number using the d.c. polarization method (Thangadurai and Weppner 2002). The evaporated gold (1·5 μm) forms the blocking electrode and the variation of conductivity of the Au/$AgCoO_2$/Au structure has been noted under a steady d.c. potential of 500 mV over a period of 30 min (figure 6). The transference number 't' is defined as

$$t = \frac{\sigma_0 - \sigma_\infty}{\sigma_0},$$

σ_0 is the conductivity at $t = 0$ and σ_∞ the saturated conductivity. The variation in conductivity is very small and the estimated transference number is 0·01 indicating that the ionic contribution to conductivity is negligible. The thermoelectric power measurement was carried out at room temperature. Figure 7 shows the result of Seebeck measurement ($S = +220\ \mu V/K$) which establishes the *p*-type nature of the carriers.

Figure 8 shows typical *J–V* characteristics of *n*-ZnO/*p*-$AgCoO_2$ *p–n* heterojunction diode grown by rf magnetron sputtering. The *J–V* characteristics of the *n*-ZnO/*p*-$AgCoO_2$ *p–n* junction diode grown by PLD is shown in the inset of figure 8. ITO/ZnO contact is ohmic (inset of figure 9). The characteristics show that the junction is rectifying. The maximum forward to reverse current ratio is about 10 at 3 V. The turn on voltage was 2 V. The diode ideality factor was determined from the slope of the forward bias, ln*I* vs *V* (figure 9). The diode does not conform to the normal forward bias *I–V* relation. The glass substrate coated with sputtered 200 nm indium tin oxide (ITO) is highly transparent (>85%) in the visible spectrum and has a conductivity, 10^{-3} Scm^{-1} (Nisha *et al* 2005). The ZnO films grown on glass substrates are highly transparent in the visible region and has hall mobility, $\mu = 6\ cm^2\ V^{-1}\ S^{-1}$; conductivity, $\sigma = 50\ Scm^{-1}$ and carrier

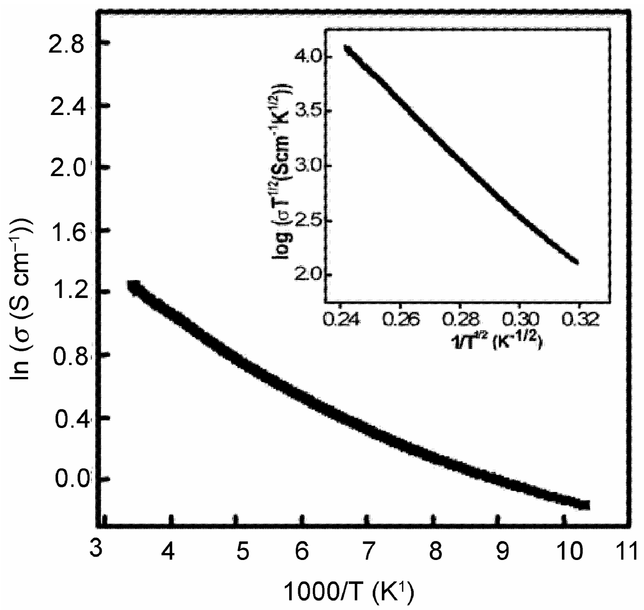

Figure 5. Conductivity log(σ) vs $1/T$ and inset shows log($\sigma T^{1/2}$) vs $1/T^{1/4}$ of the $AgCoO_2$ thin film.

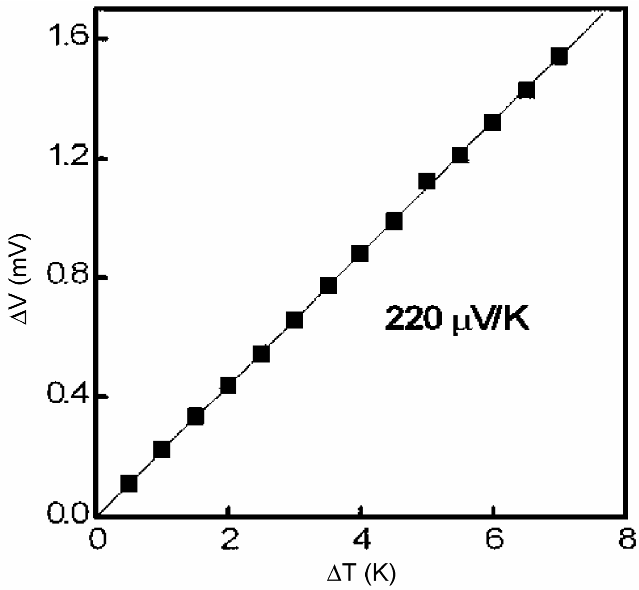

Figure 7. The plot of thermo *emf* vs temperature (ΔT).

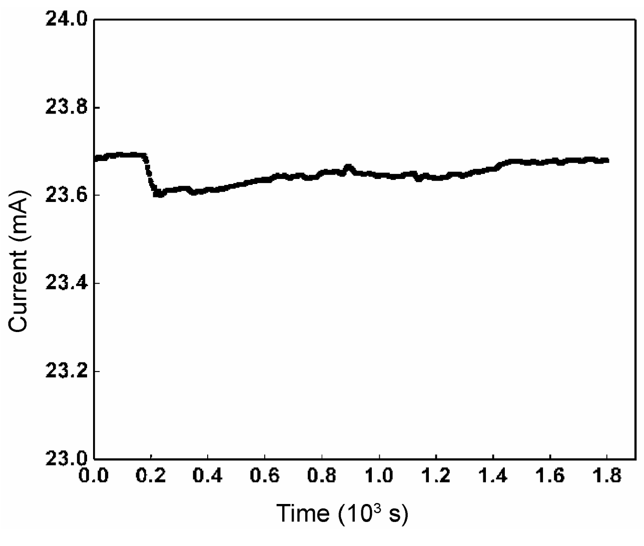

Figure 6. Variation of conductivity with time for determining transference number.

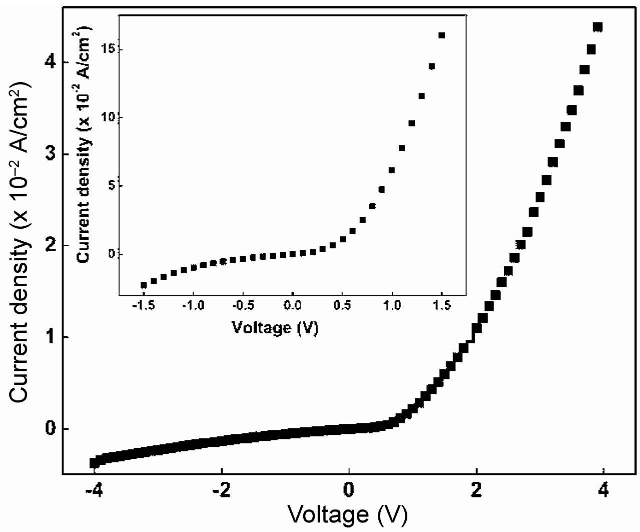

Figure 8. Current density–voltage (*J–V*) characteristics of $AgCoO_2$/ZnO *p–n* junction diode grown by rf sputtering and inset shows the *J–V* characteristics of $AgCoO_2$/ZnO *p–n* junction diode grown by PLD.

concentration, $n = 5 \times 10^{19}$ cm^{-3}. The Hall measurements on $AgCoO_2$ films could not determine the mobility of holes due to very low mobility. Thus the upper limit of mobility was assumed to be ~ 1 cm^2 V^{-1} s^{-1} and using the measured value of room temperature conductivity the carrier concentration 'n' was estimated as 1×10^{18} cm^{-3}. Based on the measured bandgap of ZnO and $AgCoO_2$, the equilibrium energy band diagram for the p-$AgCoO_2$/n-ZnO/ITO p–n heterojunction can be obtained. ITO is n-type TCO which is degeneratively doped having a bandgap of 3·6 eV with its Fermi level 'E_F' slightly above the conduction band minimum, 'E_c'. The work function of ITO is $\sim$4·7 eV (Sheats *et al* 1996), the n-type ZnO has a bandgap of 3·3 eV and an electron affinity, 4·2 eV (Siripala *et al* 2003). Assuming p-type TCO with work function 7·5 eV, bandgap being 4·15 eV and the electron affinity, $\sim$3·5 eV, band structure of the p–n heterojunction can be constructed (figure 10). The carrier concentration of the n-type ZnO is large and hence the Fermi level must be closer to the conduction band minimum while the p-type $AgCoO_2$ has large hole concentration and the Fermi level must be closer to the valence band maximum. As the p and n materials are brought into contact, a constant Fermi level will be formed at equilibrium. The expected built-in voltage based on the band diagram is $\sim$3 eV. The turn on voltage, 2 eV, is smaller than the built in potential obtained from the energy band diagram. This can be attributed to the existence of large interface defect states. The interface defect states density can be calculated from the relation (Zhang *et al* 2004)

$$N_{st} = a_2^2 - a_1^2/a_1^2 a_2^2,$$

and lattice mismatch is related to

$$\Delta a/a = 2(a_2 - a_1)/a_1^2 a_2^2,$$

where a_1 and a_2 are the lattice constants of ZnO and $AgCoO_2$, respectively. Both ZnO and $AgCoO_2$ films are highly oriented. The X-ray diffraction of ZnO shows only (002) reflection while the X-ray diffraction of $AgCoO_2$ films shows only (001) reflections. This suggests that both ZnO and $AgCoO_2$ films are highly oriented with their c-axis perpendicular to the substrates.

At very small voltages the ideality factor, $n = 8$. In the interim voltage, $n = 27$ and higher voltage, $n = 60$. The high value of ideality factor in the p-$AgCoO_2$/n-ZnO p–n junction can be attributed to poor interface and defect at the interface. Beyond 2 V, high value of ideality factor could be also due to series resistance ($1{\cdot}33 \times 10^4$ ohm). According to Wang *et al* (2004), the heterojunction diode can be modeled in different bias ranges by a series of diode or resistance. The ideality factor of the device is the sum of ideality factors of the individual junction and may lead to ideality factor much greater than two.

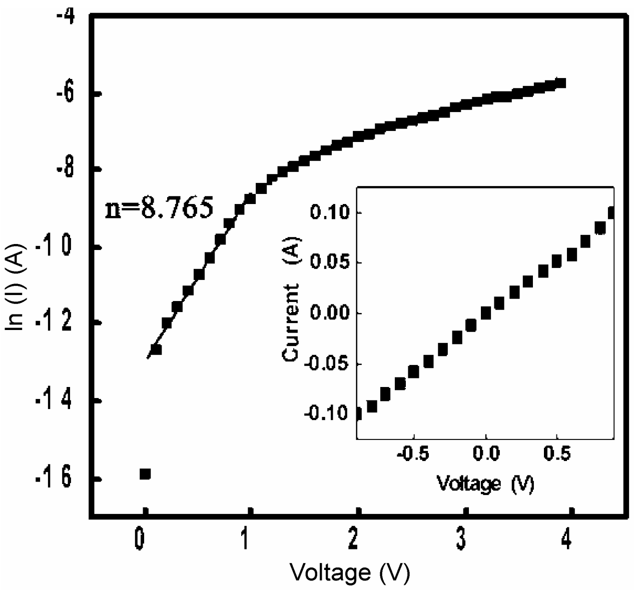

Figure 9. ln(I) vs V plot for determining the ideality factor and inset shows the I–V characteristics of ZnO/ITO contact.

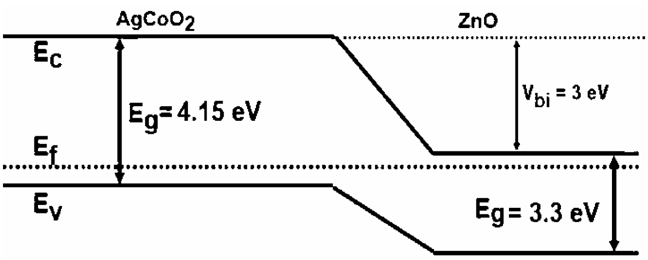

Figure 10. Equilibrium energy band diagram of the p–n heterojunction diode fabricated by rf sputtering.

4. Conclusions

In conclusion, highly c-axis oriented $AgCoO_2$ thin films with 50% transparency in the visible region were deposited on single crystalline Al_2O_3 and amorphous silica substrates by rf magnetron sputtering. The growth of crystalline $AgCoO_2$ films was unsuccessful by PLD technique. p-Type conductivity of $AgCoO_2$ was demonstrated by fabricating transparent p–n junction diode with p-$AgCoO_2$ and n-ZnO : Al thin films grown by sputtering. The junction thus obtained was found to rectify with a forward to reverse current of about 10 at an applied voltage of 3 V. Ideality factor of the diode was found to be > 1, which could be attributed to the presence of interface defect states. Though highly oriented crystalline films were able to grow by rf magnetron sputtering, the junction characteristics was almost similar to that of PLD grown amorphous $AgCoO_2$ films.

Acknowledgements

The authors thank the Kerala State Council for Science, Technology and Environment (KSCSTE) for financial support under SARD scheme. One of the authors (KAV) wishes to thank the Department of Science and Technology, New Delhi, for financial assistance under women scientist scheme.

References

Ajimsha R S, Vanaja K A, Jayaraj M K, Misra P, Dixit V K and Kukreja L M 2007 *Thin Solid Films* **515** 7352

Aoki T, Hatanaka Y and Look D C 2000 *Appl. Phys. Lett.* **76** 3527

Banerjee A N and Chattopadhyay K K 2005 *Prog. Cryst. Growth & Ch.* **50** 52

Duan N, Sleight A W, Jayaraj M K and Tate J 2000 *Appl. Phys. Lett.* **77** 1325

Hoffman R L, Wager J F, Jayaraj M K and Tate J 2001 *J. Appl. Phys.* **90** 5763

Hirsch P, Howie A, Nicholson R B, Pashley D W and Whelan M J 1977 *Electron microscopy of thin crystals* (ed.) Robert Krieger (New York: Huntington) Ch. 5

Jayaraj M K, Draeske A D, Tate J and Sleight A W 2001 *Thin Solid Films* **397** 244

Jayaraj M K, Aldrin Antony and Manoj R 2002 *Bull. Mater. Sci.* **25** 227

Jshin Y, Kwak J H and Yoon S 1997 *Bull. Korean Chem. Soc.* **18** 775

Kawazoe H, Yasukawa M, Hyodo H, Kurita M, Yanagi H and Hosono H 1997 *Nature* (*London*) **389** 939

Kng J S, Kwak J H, Shin Y J, Han S W, Kim K H and Min B I 2002 *Phys. Rev.* **B61** 10682

Kubelka P 1948 *J.Opt. Soc. Am.* **38** 448

Kubelka P and Munk F 1931 *Z. Tekh. Phys.* **12** 593

Manoj R, Pramodan P, Johny Isaac and Jayaraj M K 2003 *Proc. DAE solid state symposium* (eds) S M Sharma *et al* (New Delhi: Allied Publishers Pvt. Ltd) **46** p. 249

Mott N F 1974 *Metal–insulator transitions* (London: Taylor and Francis)

Nie X, Wei S H and Zhang S B 2002 *Phys. Rev. Lett.* **88** 66405

Nisha M, Anusha S, Aldrin Antony, Manoj R and Jayaraj M K 2005 *Appl. Surf. Sci.* **252** 1430

Ohta H, Kawamura K, Orita M, Hirano M, Sarkura N and Hosono H 2000 *Appl. Phys. Lett.* **77** 475

Otabe T, Ueda K, Kudoh A, Hosono H and Kawazoe H 1998 *Appl. Phys. Lett.* **72** 1036

Sato H, Minami T, Takata S and Yamada T 1993 *Thin Solid Films* **236** 27

Sheats J R, Antonisadis H, Hueshen M, Lenoard W, Miller J, Moon R, Roitman D and Stoking A 1996 *Science* **273** 884

Siripala W, Ivanovskaya A, Jaramillo T F, Baeck S H and McFarland E W 2003 *Sol. Energy Mater. Sol. Cells* **77** 229

Stahlin W, Oswald H R and Anrg Z 1970 *Allg. Chem.* **373** 69

Subrahmanyam A and Barik U K 2005 *J. Phys. Chem. Solids* **66** 817

Thangadurai V and Weppner W 2002 *Chem. Mater.* **14** 1136

Ueda K, Hase T, Yanagi H, Kawazoe H, Hosono H, Ohta H, Orita M and Hirano M 2001 *J. Appl. Phys.* **89** 1790

Wang C X, Yang G W, Liu H W, Han Y H, Luo J F, Gao C X and Zou G T 2004 *Appl. Phys. Lett.* **84** 2427

Yanagi H, Hase T, Ibuki S, Ueda K and Hosono H 2001a *Appl. Phys. Lett.* **78** 1583

Yanagi H, Ueda K, Ohta H, Orita M, Hirano M and Hosono H 2001b *Solid State Commun.* **12** 15

Yu P Y and Cardona M 1996 *Fundamentals of semiconductor physics and material properties* (Berlin: Springer)

Zhang D K, Liu Y C, Liu Y L and Yang H 2004 *Physica* **B351** 178